Picosecond superradiance in a three-photon resonant medium

Gombojav O. Ariunbold,[1,2] Wenlong Yang,[1,*] Alexei V. Sokolov,[1] Vladimir A. Sautenkov,[1,3] and Marlan O. Scully[1,4,5]
[1]*Institute for Quantum Studies and Department of Physics, Texas A&M University, College Station, Texas 77843, USA*
[2]*College of Optical Sciences, The University of Arizona, Tucson, Arizona 85721, USA*
[3]*Joint Institute for High Temperatures, Russian Academy of Sciences, 13, Building 2, Izhorskaya Street, Moscow 125412, Russia*
[4]*Applied Physics and Materials Science Group, Princeton University, Princeton, New Jersey 08544, USA*
[5]*Max-Planck-Institute für Quantenoptik, D-85748 Garching, Germany*
(Received 26 July 2011; published 27 February 2012)

We investigate picosecond cooperative emission in an ensemble of rubidium atoms coherently excited by 100-fs laser pulses that are three-photon resonant to the $6P$-$5S$ transition. The emitted 420-nm light is recorded by a streak camera with 2-ps resolution. The resultant pulse shape shows ringing typical for superradiance in extended sample. The pulse shape is measured as a function of input power and is compared to the solutions of Maxwell-Bloch equations. The observed superradiance, which is in the low-excitation regime, is found to be closely related to optical precursor behavior.

DOI: 10.1103/PhysRevA.85.023424 PACS number(s): 42.50.Nn, 42.65.Ky, 42.25.Bs

I. INTRODUCTION

When atoms in an ensemble are prepared in a superposition of two eigenstates and a radiative transition between these states is allowed, the ensemble is expected to cooperatively emit a pulse of light. This emission will occur on a time scale much shorter than the single-atom spontaneous emission time, and the pulse shape will be determined by properties of the ensemble as a whole, such as its total number of atoms. This type of cooperative emission, called superradiance, was predicted by Dicke for samples whose size is much smaller than the light wavelength [1]; later, the concept of superradiance was extended to long samples where phase matching comes into play [2]. Superradiance, which occurs due to the presence of coherent excitation, is often viewed as part of the superfluorescence process, which develops from an initially incoherent population-inverted state [3,4]. In superfluorescence, ensemble coherence builds up spontaneously. However, initial coherence can also be set up by an external driving field, i.e., through a coherent multiphoton excitation. The resultant superradiance, in turn, will have an effect on subsequent field-atom interaction.

To the best of our knowledge, no experiment on picosecond time-resolved study of the multiphoton-excited cooperative emission has been reported. Recent technological advances, for example in ultrafast lasers and streak cameras, have made time-resolved study on the above-mentioned topic feasible on a picosecond time scale. A picosecond time-resolved study of other types of cooperative emissions in atomic vapor, i.e., superfluorescence, was accomplished in our recent work [5–9]. Some of this work [6] extended the application of cooperative emission further to coherent UV light generation.

In this paper, we study superradiance in a three-photon resonant medium in the picosecond regime. A rubidium vapor and ultrafast streak camera were used in our experiment. The observed superradiance pulses exhibit temporal ringing, which is one of the intriguing features of the cooperative processes. In order to gain insight into the generation process, we perform a simulation using theory similar to the one used in [4]. We adapt the Maxwell-Bloch equations [10] and include the coherent and weak three-photon excitation to calculate the superradiance pulse shape in the focal region of pump laser. Thereafter, the superradiance pulse is treated as propagating linearly through the rest of the resonant medium. The present theory also suggests a connection between superradiance in a three-photon resonant medium and Sommerfeld-Brillouin precursors [11–13]: as the short superradiant pulse propagates through the resonant medium beyond the focal point, it undergoes a shape transformation somewhat akin to formation of optical precursors.

This paper is organized as follows. The next section explains the details of our experiment. In Sec. III, we show the experimental results and present the corresponding theory and discussions. The last section gives conclusions.

II. EXPERIMENTAL SETUP

In this section we list the details of the experiment. A diagram of the experimental setup is shown in Fig. 1(a). The input laser pulses had about 100-fs time duration with a 1-kHz repetition rate and were furnished by the conventional Ti:sapphire femtosecond laser system, which consists of an oscillator, regenerative amplifier, and two optical parametric amplifiers (OPAs). The input laser pulses were focused by a lens ($f = 10$ cm) into a 7-cm-long Rb cell. The cell was made of a sapphire body and had garnet windows able to withstand high temperature. The cell was operated at a temperature of about 204°C and provided 9×10^{14} atoms/cm^3. The center wavelength of the input laser from one OPA was tuned to $\lambda_{in} = 1260$ nm, which was three-photon resonant to the $6P$-$5S$ transition of rubidium atoms; see Fig. 1(b). The bandwidth of the 1260-nm light is about 19 nm, which corresponds to a 120-fs (full width at half maximum) Gaussian pulse. The coherently excited atoms emitted light centered at 420 nm in the direction of the input laser field. A reference beam at 778 nm furnished by another OPA was used as a time reference for all pulses recorded by the streak camera. Note that the cell also provided an absolute time reference in addition to producing the 420-nm light. To accomplish this task, the input beam's center wavelength was

*ywlonion@hotmail.com

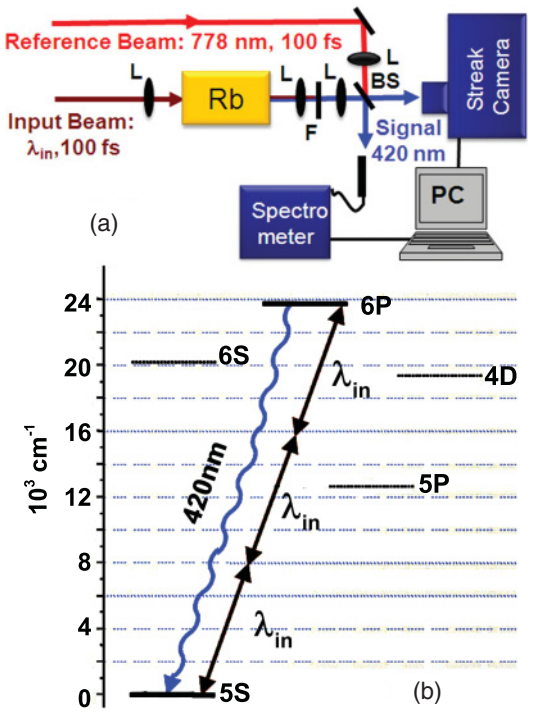

FIG. 1. (Color online) (a) Schematics of the experimental setup. Rb, rubidium vapor cell and oven; L, lens; F, filter to remove the residue of the input laser light; BS, thin glass plate (beam splitter); PC, computer. The input light was furnished by a commercial femtosecond laser system. The laser's center wavelength was tuned to $\lambda_{in} = 1260$ nm. The produced 420-nm light was recorded by both the streak camera and the spectrometer. The Rb cell was heated to and kept at about 204°C, and atomic density was approximately 9×10^{14} cm^{-3} at this temperature. (b) Rb atomic level scheme. Rb atoms were excited via a three-photon transition from $5S$ to $6P$. The atoms emitted light at 420 nm on the $6P$-$5S$ transition.

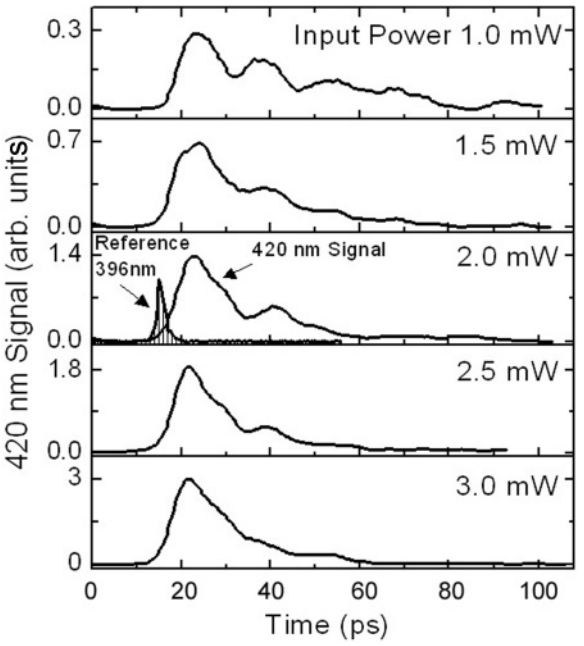

FIG. 2. The streak camera data for the 396-nm reference (curve with hatch marks) and 420-nm superradiance pulses. The input 1260-nm beam power was varied from 1 to 3 mW.

tuned to $\lambda_{in} = 1188$ nm to produce the third harmonic at 396 nm while the experimental setup remained unchanged. In this off-resonant case where the cooperative effect was negligible, the third harmonic signal was generated instantaneously. Thus, the 396-nm signal was used as a reference pulse for measuring the delay between superradiance pulses at 420 nm and the input 1260-nm pulses. Since 396-nm pulses were much shorter than the temporal resolution of the streak camera, this measurement also indicated the resolution of the streak camera.

III. RESULTS AND DISCUSSIONS

The main experimental results are summarized in Fig. 2. The 396-nm reference pulses were recorded at an input laser power of 4 mW. The 396-nm reference pulses were averaged up to 100 laser shots. The averaged 396-nm reference pulse is included in the graph. The recorded data for the 420-nm pulses were first averaged for up to 100 laser shots and then smoothed by the adjacent-averaging method using up to 20 data points, which corresponds to about 4 ps. The data, after the aforementioned processing, are shown in Fig. 2.

The measured 420-nm pulse, in general, has a steep rising edge with a moderately long tail. No measurable delay was observed between the 396-nm reference and 420-nm pulses; i.e., the macroscopic dipole of the medium was produced quasi-instantaneously by the 100-fs input laser pulses. The slope of the rising edge of the 420-nm pulse was relatively short and independent of input power. In contrast, the pulse tail part was long, and its duration and shape changed as the input power varied. The total time duration of the 420-nm pulse was of a few tens of picoseconds and much shorter compared to the fluorescence lifetime (0.36 μs on the $6P$-$5S$ transition). The atomic coherence dephasing and other incoherent relaxation processes were negligible on this time scale. The reduction of the temporal ringing of the 420-nm pulse was observed as input power increased.

The peak intensity of the 420-nm pulse for different input powers in Fig. 2 demonstrated a nonlinear dependence [as shown in Fig. 4(a)]. It is compared with a curve of the form aP_{input}^3, where $a = 0.12$ and P_{input} is the input power in milliwatts. The cubic power dependence of the output pulse peak intensity is expected for pure third-order excitation.

The temporal ringing, clearly observed in our experiment, is common in cooperative processes [3,14,15], where the atoms are initially fully excited. However, in our experiment, the excitation is weak. The pump power of the 1260-nm beam varied from 1 to 3 mW. The pulse area for a pulse at 1-mW input laser power is about 0.04 (1 mW average laser power corresponds to 1 μJ pulse energy). The atoms are weakly excited via a three-photon process for such a small input power. The ringing in the pulse shape and especially its change for different input laser powers are intriguing and quite unexpected. To gain an understanding of the underlying process, we performed a simulation with $(1 + 1)$-dimensional (one time and one space) Maxwell-Bloch equations.

We performed simulations in two steps. The first step is similar to the theory used in [4], but the excitation is a three-photon process. In the second step of the simulation, the superradiance pulse generated in first step propagates linearly through the rest of the Rb vapor. This scheme is related to the fact that the laser powers used in our experiment were low, and the probability of three-photon excitation nonlinearly depended on input laser power. Considering the laser intensity is much smaller outside than that inside the focal region, we assume, in the simulation, that only those atoms in the focal region were excited by the 1260-nm laser through three-photon excitation and the generated 420-nm pulse propagated through the rest of the Rb cell without any perturbation from the 1260-nm laser pulses. In the simulation, we chose the pulse duration of the input laser and the length of focal region to be 120 fs and 3.6 mm, respectively.

The superradiant pulse shape generated within the focal region can also be found analytically [1]: $I_{SR}(t) \simeq \mathrm{sech}^2[\alpha(t - t_0)]\theta(t)$, where α is proportional to number density of the atoms, $\theta(t)$ is Heaviside step function, and t_0 depends on initial coherence of atoms and on the population inversion. For weakly excited atoms, t_0 is a large negative number, and the pulse shape is close to the form $I_{SR}(t) \simeq \exp[-2\alpha t]\theta(t)$. Our numerical simulation gives a slightly different pulse shape in Fig. 3(a). In addition to the generated intensity (solid line), we plot the field amplitude (dashed line), and we see that at $t > 100$ ps it becomes negative. This pulsed field reshaping is due to finite absorption of Rb vapor within the focal region. As this pulse propagates through the rest of the Rb cell, it is further distorted and acquires an oscillating tail, as shown in Fig. 3(b). After the resolution of the streak camera is taken into account and data processing smoothing is considered, the pulse shape becomes smooth, as shown in the inset in Fig. 3(b). It is interesting to point out that propagation of a pulse with such an abrupt rising edge, like the one in Fig. 3(a), through a two-level resonant medium will generate optical precursors. This problem was discussed by Sommerfeld and Brillouin 100 years ago [11,12] to test whether the speed of light in absorptive media can exceed the speed of light in vacuum.

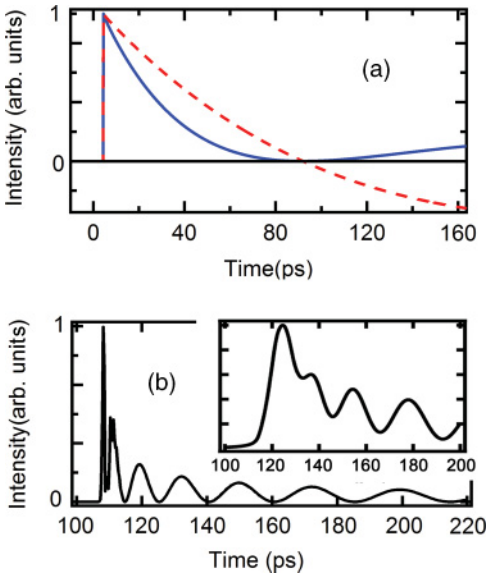

FIG. 3. (Color online) (a) The solid line is the pulse shape (electric field intensity) generated in the focal region in the rubidium cell. The dashed line is the corresponding electric field of the generated pulse. (b) The pulse shape (electric field intensity) after the pulse in (a) is transmitted through the rest of the rubidium cell. The inset shows the pulse shape (electric field intensity) after the resolution of the streak camera and averaging in data processing are taken into account.

In our simulation, the distance of propagation for the generated 420-nm light (after the focal region) was varied within a reasonable range to fit experimental data for different pump powers. The output pulses from the rubidium cell were further convolved with the instrumental function taking into account a 2-ps temporal resolution of the streak camera. Finally the pulse was further smoothed by averaging 20 adjacent points, which covered an interval of about 7 ps. The details of the simulation can be found in [16]. The calculated superradiant pulse shape did not change noticeably when we varied the excitation amplitude (from 1 to 3 mW in excitation power) and/or the length of the focal region between 50 μm and 3.6 mm, as long as its pulse area was much smaller than π. In this small excitation limit, the pulse shape's invariance with respect to these parameters is as expected from the analysis of the Maxwell-Bloch theory. In contrast to this expectation, the experimentally measured output pulse shapes changed significantly as the pump power was varied, even though the excitation was weak.

Our naive hypothesis is that the pump beam's focal point inside the Rb cell was possibly altered as a result of nonlinear propagation. Indeed, as we varied the propagation length of the superradiant pulse, the calculated pulse shape changed. The simulation result is shown in Fig. 4(b). For the experimental data for 1-mW pump power, a simulation with a propagation length of 23 mm fits the data well. The experiment data for 2-mW pump power can be fitted by choosing the propagation length to be 35 mm in the simulation.

As noted above, the 420-nm light generated in the focal region has a sharp rising edge and a long trailing edge. The

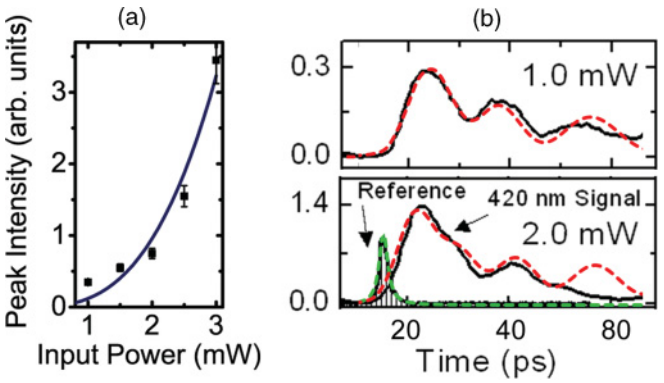

FIG. 4. (Color online) (a) The peak intensity of the measured pulses for different powers (the squares with error bars showing the data range before averaging) and a curve of the form aP_{input}^3, with $a = 0.12$ (solid curve). (b) The measured pulse shapes (solid curves) for 1- and 2-mW input powers and the theoretical results by numerically solving Maxwell-Bloch equations (dashed curves). In the calculation, for the 1-mW (2-mW) data, we used 23 mm (35 mm) as the propagation length from the focal point of the pump beam to the end of the rubidium cell.

rise time of hundreds of femtoseconds is set by the duration of the pump pulse. The trailing edge is hundreds of picoseconds long. The propagation of the pulse with such a temporal shape in the resonant medium fulfills the condition of generating optical precursors [11–13]. Therefore, the ringing in the pulse shape in Fig. 4(b) can also be understood as the generation of optical precursors, where the optical precursor is the first pulse, and the following shape is the delayed so-called main pulses. Similar pulse shapes have been recognized as optical precursors and main pulses in several different media [17,18].

IV. CONCLUSIONS

To conclude, the cooperative emission was observed in the three-photon resonant medium, Rb atomic vapor, pumped by 100-fs pulses. Temporal ringing was observed in the pulse shapes measured by the streak camera for different input powers. By solving Maxwell-Bloch equations, we can explain the ringing in the observed pulse shape. The explanation of pulse-shape variance due to a change in pump power deserves further development in the theory. The relation between the superradiance and optical precursor is shown.

We believe that this experimental work will be of interest to stimulate the further discussion that cooperative emissions can play an important role in resonance-enhanced multiphoton ionization (REMPI) [22–27]. A typical method to produce the frequency upconversion of the input IR light is based on multiphoton nonlinear processes. Considerable interest has been devoted to the frequency upconversion in alkali-metal vapors [6,19–21]. In this context, the cooperative emission resulting from the frequency upconversion may be of interest.

ACKNOWLEDGMENTS

The authors thank M. Kash, H. Li, Y. Rostovtsev, G. Welch, L. Yuan, and B. Strycker for their fruitful discussions. This work was supported by NSF Grant No. EEC-0540832 (MIRTHE ERC), NSF Grant No. 722800, the Office of Naval Research, the Army Research Office (Grant No. W911NF-07-1-0475), the Robert A. Welch Foundation (Grants No. 1261 and No. 1547), and the Herman F. Heep and Minnie Belle Heep Texas A&M University Endowed Fund held and administered by the Texas A&M Foundation.

[1] R. H. Dicke, Phys. Rev. **93**, 99 (1954).
[2] N. E. Rehler and J. H. Eberly, Phys. Rev. A **3**, 1735 (1971).
[3] N. Skribanowitz, I. P. Herman, J. C. MacGillivray, and M. S. Feld, Phys. Rev. Lett. **30**, 309 (1973).
[4] J. C. MacGillivray and M. S. Feld, Phys. Rev. A **14**, 1169 (1976).
[5] G. O. Ariunbold, M. M. Kash, V. A. Sautenkov, H. Li, Yu. V. Rostovtsev, G. R. Welch, and M. O. Scully, Phys. Rev. A **82**, 043421 (2010).
[6] G. O. Ariunbold, M. M. Kash, V. A. Sautenkov, H. Li, Yu. V. Rostovtsev, G. R. Welch, and M. O. Scully, J. Opt. Soc. Am. B **28**, 515 (2011).
[7] G. O. Ariunbold, V. A. Sautenkov, and M. O. Scully, J. Opt. Soc. Am. B **28**, 462 (2011).
[8] G. O. Ariunbold, V. A. Sautenkov, and M. O. Scully, in *Conference on Lasers and Electro-optics*, OSA Technical Digest (Optical Society of America, Washington, DC, 2010), paper CMA4.
[9] G. O. Ariunbold, V. A. Sautenkov, and M. O. Scully, Phys. Lett. A **376**, 335 (2012).
[10] P. Meystre and M. Sargent III, *Elements of Quantum Optics* (Springer, New York, 2007).
[11] A. Sommerfeld, Ann. Phys. (NY) **44**, 177 (1914).
[12] L. Brillouin, Ann. Phys. (NY) **44**, 204 (1914).
[13] L. Brillouin, *Wave Propagation and Group Velocity* (Academic, New York, 1960).
[14] M. Gross, C. Fabre, P. Pillet, and S. Haroche, Phys. Rev. Lett. **36**, 1035 (1976).
[15] M. Gross and S. Haroche, Phys. Rep. **93**, 301 (1982).
[16] W. Yang, M.S. thesis, Texas A&M University, 2011.
[17] J. Aaviksoo, J. Kuhl, and K. Ploog, Phys. Rev. A **44**, R5353 (1991).
[18] D. Wei, J. F. Chen, M. M. T. Loy, G. K. L. Wong, and S. W. Du, Phys. Rev. Lett. **103**, 093602 (2009).
[19] R. B. Miles and S. E. Harris, IEEE J. Quantum Electron. **9**, 470 (1973).
[20] A. S. Zibrov, M. D. Lukin, L. Hollberg, and M. O. Scully, Phys. Rev. A **65**, 051801 (2002).
[21] A. Vernier, S. Franke-Arnold, E. Riis, and A. S. Arnold, Opt. Express **18**, 17020 (2010), and references therein.
[22] J. C. Miller, R. N. Compton, M. G. Payne, and W. R. Garrett, Phys. Rev. Lett. **45**, 114 (1980).
[23] R. N. Compton, J. C. Miller, A. E. Carter, and P. Kruit, Chem. Phys. Lett. **71**, 87 (1980).
[24] M. G. Payne, W. R. Garret, and H. C. Baker, Chem. Phys. Lett. **75**, 468 (1980).
[25] M. G. Payne and W. R. Garrett, Phys. Rev. A **26**, 356 (1982).
[26] M. Poirier, Phys. Rev. A **27**, 934 (1983).
[27] V. Peet, Phys. Rev. A **74**, 033406 (2006), and references therein.